Medical Physics
The International Journal of Medical Physics Research and Practice

# Prospects of photoacoustic tomography

Lihong V. Wang

Citation: Medical Physics **35**, 5758 (2008); doi: 10.1118/1.3013698
View online: http://dx.doi.org/10.1118/1.3013698
View Table of Contents: http://scitation.aip.org/content/aapm/journal/medphys/35/12?ver=pdfcov
Published by the American Association of Physicists in Medicine



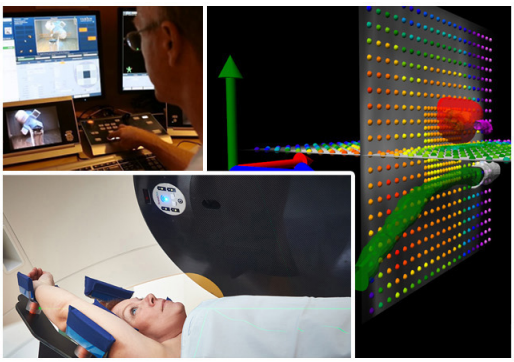



# Prospects of photoacoustic tomography

Lihong V. Wang[a)]
*Optical Imaging Laboratory, Department of Biomedical Engineering, Washington University in St. Louis, Campus Box 1097, One Brookings Drive, St. Louis, Missouri 63130-4899*

(Received 8 August 2008; revised 10 October 2008; accepted for publication 15 October 2008; published 19 November 2008)

Commercially available high-resolution three-dimensional optical imaging modalities—including confocal microscopy, two-photon microscopy, and optical coherence tomography—have fundamentally impacted biomedicine. Unfortunately, such tools cannot penetrate biological tissue deeper than the optical transport mean free path (~1 mm in the skin). Photoacoustic tomography, which combines strong optical contrast and high ultrasonic resolution in a single modality, has broken through this fundamental depth limitation and achieved superdepth high-resolution optical imaging. In parallel, radio frequency-or microwave-induced thermoacoustic tomography is being actively developed to combine radio frequency or microwave contrast with ultrasonic resolution. In this Vision 20/20 article, the prospects of photoacoustic tomography are envisaged in the following aspects: (1) photoacoustic microscopy of optical absorption emerging as a mainstream technology, (2) melanoma detection using photoacoustic microscopy, (3) photoacoustic endoscopy, (4) simultaneous functional and molecular photoacoustic tomography, (5) photoacoustic tomography of gene expression, (6) Doppler photoacoustic tomography for flow measurement, (7) photoacoustic tomography of metabolic rate of oxygen, (8) photoacoustic mapping of sentinel lymph nodes, (9) multiscale photoacoustic imaging *in vivo* with common signal origins, (10) simultaneous photoacoustic and thermoacoustic tomography of the breast, (11) photoacoustic and thermoacoustic tomography of the brain, and (12) low-background thermoacoustic molecular imaging. © *2008 American Association of Physicists in Medicine*. [DOI: 10.1118/1.3013698]

Key words: microscopy, melanoma detection, endoscopy, functional imaging, molecular imaging, reporter gene imaging, Doppler effect, metabolic rate of oxygen, sentinel lymph nodes, multiscale imaging, thermoacoustic tomography, breast imaging, brain imaging

## I. INTRODUCTION

The field of photoacoustic tomography (PAT) has grown a great deal in the past few years. PAT is cross-sectional or three-dimensional imaging based on the photoacoustic effect. Alexander Graham Bell first reported on the photoacoustic effect in 1880. Only recently, however, was PAT developed as an imaging technology.[1–29] PAT combines high ultrasonic resolution and strong optical contrast in a single modality, capable of providing high-resolution structural, functional,[19] and molecular[30,31] imaging *in vivo* in optically scattering biological tissue at new depths.

In biological tissues, light transfer is dominated by scattering. The mean free path is on the order of 0.1 mm, and the transport mean free path is on the order of 1 mm. While the former measures the frequency of predominantly anisotropic scattering, the latter assesses the frequency of equivalent isotropic scattering. As a result of scattering, photon propagation transitions from the ballistic regime into the diffusive regime around one transport mean free path.[4] Specifically, the ballistic regime is within the mean free path, where a significant number of photons have undergone no scattering. The quasiballistic regime is from the mean free path to the transport mean free path, where photons have sustained a few scattering events but retain a strong memory of the original incidence direction. The quasidiffusive regime is from the transport mean free path to ten times the transport mean free path, where photons have sustained many scattering events and retain only a weak memory of the original incidence direction. The diffusive regime is beyond ten times the transport mean free path, where photons have suffered many scattering events that they have almost completely lost their memory of the original incidence direction.[4]

Two important depth limits exist for optical imaging. One is near the optical transport mean free path, representing the depth of the quasiballistic regime in biological tissue. Ballistic light intensity attenuates exponentially with a decay constant equal to the mean free path. To reach one transport mean free path deep, photons must undergo significant scattering, making focusing ineffective.[32] We refer to this barrier as the soft depth limit for high-resolution optical imaging. Another depth limit is around 50–70 mm, which equals roughly ten times the $1/e$ optical penetration depth (the reciprocal of the effective attenuation coefficient). To reach this depth, light must experience 43 dB or 20 000 times one-way decay in intensity. Beyond this limit, even diffuse photons are too few for practical purposes. We refer to this limit as the hard depth limit for optical imaging. Nevertheless, if the tissue is illuminated from opposite sides, a thickness greater than 10 cm can be potentially covered, which is adequate for many biomedical applications such as breast imaging.

High-resolution optical imaging beyond the soft depth limit, sometimes referred to as superdepth optical imaging, remained a void until PAT was developed. None of the commercially available optical ballistic imaging modalities—including confocal microscopy, two-photon microscopy and optical coherence tomography—can penetrate into scattering biological tissue beyond the soft depth limit. By contrast, diffuse optical tomography—based on multiple-scattered photons—can provide rapid functional and molecular imaging beyond the soft depth limit; however, it has poor spatial resolution. The motivation driving the development of PAT is to overcome the poor spatial resolution of diffuse optical tomography or the soft depth limit of existing high-resolution optical imaging.

An approach to overcome the optical hard depth limit is to adopt radiofrequency or microwaves for photoacoustic excitation.[6,7] In this case, the technology is referred to as radio frequency- or microwave-induced acoustic tomography or thermoacoustic tomography (TAT). For simplicity here, radio frequency refers to microwaves as well. In TAT, a radio frequency generator instead of a laser is used. The radio frequency generator transmits radio frequency pulses into the tissue to be imaged. Radio frequency absorption produces heat and subsequent ultrasonic waves. The ultrasound detection and image formation are similar to those in PAT.

Both PAT and TAT are designed to overcome the poor spatial resolution of pure optical or radio frequency imaging yet to retain the high electromagnetic contrasts. In terms of spatial resolution, pure optical imaging beyond the soft depth limit suffers from strong diffusion due to tissue scattering, whereas pure radio frequency imaging suffers from strong diffraction due to the long wavelength. Ultrasonic scattering coefficient in tissue is 2–3 orders of magnitude less than the optical counterpart, and the acoustic diffraction (or wavelength) is 2–3 orders of magnitude weaker (or shorter) than the radio frequency counterpart. As a result, PAT and TAT can provide high spatial resolution by detecting the induced ultrasonic waves. Unlike ultrasonography or optical coherence tomography, PAT and TAT produce speckle-free images.

The subsequent sections are organized as follows. First, the basic principle of PAT is reviewed. Then, the future prospects of PAT and TAT are envisioned on twelve specific topics. Finally, a summary is provided.

## II. BASICS OF PHOTOACOUSTIC TOMOGRAPHY

PAT involves optical irradiation, ultrasonic detection, and image formation. The tissue is usually irradiated by a short-pulsed laser beam to produce thermal and acoustic impulse responses. Locally absorbed light is converted into heat, which is further converted to a pressure rise via thermoelastic expansion of the tissue. The initial pressure rise—determined by the local optical energy deposition (also called specific optical absorption in the unit of $J/m^3$) and other thermal and mechanical properties—propagates in the tissue as an ultrasonic wave, which is referred to as a photoacoustic wave. The photoacoustic wave is detected by ultrasonic transducers placed outside the tissue, producing electric signals. The electric signals are then amplified, digitized, and transferred to a computer, where an image is formed. PAT depends on any absorbed photons, either unscattered or scattered, to produce photoacoustic signals as long as the photon excitation is relaxed thermally. Readers are referred to recent review and tutorial articles for more details.[1,4]

The formation of a photoacoustic image, mapping the photoacoustic source according to the detected sound signals, can be exemplified with the simplest case of pinpointing a single sound source such as thunder in three-dimensional (3D) space. If the time delay between seeing lightening and hearing thunder is recorded, one can infer that the thunder took place on a spherical surface of a radius determined by the product of the speed of sound and the time delay. If three such measurements are taken at different locations, the sound source can be accurately triangulated. If produced by the photoacoustic effect, the sound source can be imaged by PAT. In most practical cases, the sound source is spatially distributed rather than localized at a point.

PAT has been implemented in two major forms. One form is based on a scanning focused ultrasonic transducer. Acoustic focusing in combination with time-resolved detection of photoacoustic waves directly provides 3D spatial resolution. Scanning over the tissue produces tomographic images. Dark-field confocal photoacoustic microscopy belongs to this category.[33–35] Dark field means that the light illumination pattern on the tissue surface is donut shaped with a dark core; confocal means that the ultrasonic detection shares the same focus as the light illumination. The other form is based on an array of unfocused ultrasonic transducers. This method, also referred to as photoacoustic computed tomography, requires the use of an inverse algorithm to reconstruct a tomographic image.[36]

The dominant contrast of interest is based on the optical absorption in the photoacoustic excitation phase. By using multiwavelength measurement, one can simultaneously quantify concentrations of multiple chromophores of different colors, such as oxygenated and deoxygenated hemoglobin molecules in red blood cells. Such quantification of hemoglobin can provide functional imaging of the concentration and oxygen saturation of hemoglobin. Both parameters are related to hallmarks of cancer: the concentration of hemoglobin correlates with angiogenesis,[27] whereas the oxygen saturation of hemoglobin correlates with hypermetabolism.[31] Such parameters of hemoglobin can also be used to image brain activity.[19] In addition, extrinsic optical absorption contrast agents can be used to provide molecular imaging of biomarkers.[30,31]

PAT is highly sensitive to optical absorption. PAT works on dark background—when no absorption exists, the background signal is zero. Such dark background enables sensitive detection. In the presence of absorption, the foreground signal is proportional to the absorption coefficient. Any small fractional change in optical absorption coefficient translates into an equal amount of fractional change in PAT signal, which means a relative sensitivity of 100%.[2] When the frac-

tional change is large, light transport modeling can be used to quantify the optical absorption coefficient.[37]

The spatial resolution is derived from ultrasonic detection in the photoacoustic emission phase. Ultrasonic scattering is much weaker than optical scattering. The wavelength of the detected photoacoustic wave is sufficiently short. As a result, photoacoustic waves provide better resolution than optical waves beyond the soft depth limit. Among other parameters, the center frequency and the bandwidth of the ultrasonic detection system predominantly determine the spatial resolution of PAT. The greater the center frequency and the wider the bandwidth, the better the spatial resolution is.

## III. PREDICTIONS

### III.A. Photoacoustic microscopy of optical absorption going mainstream

Prediction 1: Photoacoustic microscopy will join the suite of mainstream optical microscopy technologies.

Photoacoustic microscopy (PAM) has shown the following capabilities. First, PAM has broken through the current fundamental depth limitation of high-resolution optical imaging modalities.[33,34] The commercially available microscopic optical imaging modalities—including confocal microscopy, two-photon microscopy, and optical coherence tomography—cannot provide penetration into scattering biological tissue beyond the soft depth limit (~1 mm in the skin) because they are based on ballistic and quasiballistic photons. Taking advantage of photons that have been scattered an any number of times, PAM has filled the void of penetration and reached superdepth optical imaging. As will be shown in Sec. III A, imaging depths of 3–30 mm have been experimentally demonstrated. Second, the depth-to-resolution ratio (maximum imaging depth divided by the axial resolution) can be approximately maintained at more than 100 while the imaging depth and spatial resolution are scaled. Third, PAM provides functional imaging based on physiologically specific endogenous optical absorption contrasts. The red color in Fig. 1 shows a PAM image of blood vasculature using endogenous contrast only, the contrast between the blood and the background is as high as 13:1.[34] In comparison, other imaging modalities such as x-ray computed tomography and magnetic resonance imaging usually require the use of exogenous contrast agents to image blood vessels clearly with high contrast. Further, magnetic resonance imaging cannot measure the concentration of hemoglobin and the absolute oxygenation of hemoglobin. Fourth, PAM can provide molecular or genetic imaging based on exogenous contrast mechanisms.[30,31] Fifth, PAM can be constructed to image in real time. A *B*-scan frame rate of 50 Hz has been achieved.[38,39] Sixth, PAM images are free of speckle artifacts. Finally, PAM is safe to human subjects and ready for clinical applications.

The various high-resolution optical imaging modalities are compared in Table I. While PAM is sensitive to optical absorption, it is insensitive to optical scattering or fluorescence.[2] The various modalities complement each other in both penetration and contrast; they will therefore coexist.

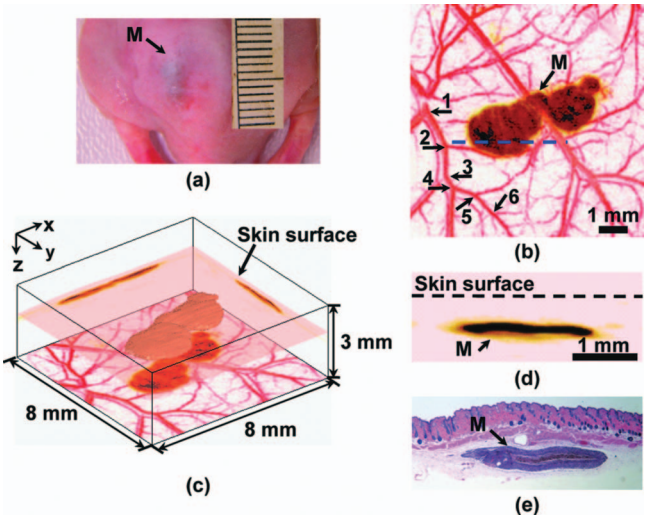


FIG. 1. (a) Photograph of a melanoma in a nude mouse; (b) image acquired with the 50-MHz photoacoustic microscope operating at 584 and 764 nm. Composite of the two maximum amplitude projection (MAP) images projected along the *z* axis. Six orders of vessel branching (1–6) can be observed. (c) 3D rendering of the melanoma image acquired at 764 nm. Two MAP images at this wavelength projected along the *x* and *y* axes are shown on the sidewalls. The composite image in panel b is redrawn at the bottom. The top of the tumor is 0.32 mm below the skin surface, and the thickness of the tumor is 0.3 mm. (d) Close-up two-dimensional image of the melanoma in a cross-section parallel with the *z*-*x* plane at the dashed line in panel b. (e) HE-stained histological section at the same marked location. *M*: melanoma. Reproduced with permission (Fig. 2 of Ref. 34).

In light of its appealing capabilities, PAM is expected to become commercially available and widely used in biomedical research and clinical practice.

### III.B. Melanoma detection using photoacoustic microscopy

Prediction 2: Melanoma detection will become a high impact application of photoacoustic microscopy.

While melanoma is the most deadly form of skin cancer, it is curable if detected early. The diagnosis of melanoma is often based on its appearance. Abnormally appearing skin lesions are resected for biopsy. Because visual inspection is inaccurate and biopsy is invasive, an accurate noninvasive method of melanoma detection is desirable.

PAM can acquire (1) structural images measuring tumor burden and depth, (2) functional images of hemoglobin concentration measuring tumor angiogenesis—a hallmark of cancer, (3) functional images of hemoglobin oxygen saturation ($SO_2$) measuring tumor hypoxia or hypermetabolism—another hallmark of cancer, and (4) images of melanin concentration measuring tumor pigmentation—a hallmark of melanotic melanoma, consisting of >90% of melanomas (note that even amelanotic melanoma contains a low concentration of melanin). An *in vivo* PAM image of a melanoma in a small animal is shown in Fig. 1. The depth of melanoma, also an important prognostic parameter, was measured by PAM. By contrast, other high-resolution optical microscopy technologies cannot provide the required penetration. Because of biological variability in most biological problems, a

TABLE I. Comparison of high-resolution optical imaging modalities.

| Modality | Penetration | Primary contrast |
|---|---|---|
| Confocal microscopy | ~0.5 mm | Scattering, fluorescence |
| Two-photon microscopy | ~0.5 mm | Fluorescence |
| Optical coherence tomography | ~1 mm | Scattering, polarization |
| Photoacoustic microscopy | Up to 30 mm, scalable | Absorption |

single biomarker is unlikely able to provide accurate diagnosis. However, the combination of four complementary measures can significantly enhance the likelihood of high accuracy. In addition, as Doppler photoacoustic microscopy matures, blood flow measurement can add more diagnostic information. Therefore, it is expected that the combined rich contrasts will provide the sensitivity and specificity needed for the early detection of melanoma.

### III.C. Photoacoustic endoscopy

Prediction 3: Photoacoustic endoscopy will play a unique role in diagnosing gastrointestinal cancer.

Incidence of gastrointestinal cancer is on the rise yet often diagnosed at an untreatable stage. Optical endoscopy is the current practice in identifying suspicious lesions for subsequent biopsy. Operating in the mode of surface or ballistic imaging, existing optical endoscopy has severely limited penetration. Ultrasound endoscopy is being introduced into the clinic as well. Yet the mechanical contrast in ultrasound images often cannot provide the required sensitivity and specificity. Other medical imaging modalities such as x-ray computed tomography and magnetic resonance imaging have not been implemented endoscopically because of diagnostic insensitivity, technological difficulties or expenses.

Light and sound are well suited for endoscopic applications. Because both forms of energy have been used endoscopically, PAM can naturally be implemented endoscopically. As PAM can provide a multitude of endogenous contrasts at new depths, it is likely to provide accurate diagnosis of superficial as well as deep lesions in the gastrointestinal tract. Similarly, intravascular photoacoustic imaging can also be implemented.[40] Of course, adding molecular imaging capability to photoacoustic endoscopy can further enhance the diagnostic accuracy albeit at the inconvenience of using exogenous contrast agent.

### III.D. Simultaneous functional and molecular photoacoustic tomography

Prediction 4: Simultaneous functional and molecular photoacoustic tomography will provide unprecedented sensitivity and specificity to cancer diagnosis.

While functional imaging is based on endogenous contrast, molecular imaging is based on exogenous contrast—which essentially stains invisible biomarkers *in vivo*. The former maps physiological activities at the tissue or organ level, whereas the latter images biological and pathophysiological processes at the molecular level. Both can be accomplished quantitatively and noninvasively—with the exception of introducing exogenous contrast agent. By combining imaging physics with molecular and cell biology, molecular imaging can potentially lead to better methods for preventing, diagnosing, and managing diseases. For example, tumor biology and angiogenesis can be characterized with high specificity because molecular imaging probes can be designed to target at specific molecular biomarkers expressed on neoendothelial-and tumor-cell surfaces. Such characterization will accelerate the development of molecular-targeted cancer therapeutics. Nevertheless, molecular imaging will not supplant functional imaging. The former requires the use of foreign contrast agent, whereas the latter depends on intrinsic contrast only. Therefore, the former may involve some degree of toxicity and may not be universally applicable. In addition, functional imaging can measure some physiological parameters that cannot be easily measured by molecular imaging.

Simultaneous functional and molecular PAT was demonstrated in live mice (Fig. 2).[31] One million human U87 glioblastoma tumor cells were implanted stereotactically into young adult immunocompromised nude mice in the head ~3 mm below the scalp surface. One week post inoculation, 20 nmol of molecular imaging probe IRDye800-c(KRGDf) was administered through the tail vein while mannitol was used to permeabilize the blood brain barrier. Approximately 20 h later, imaging with PAT was conducted. Four laser wavelengths—764, 784, 804, and 824 nm—were used to measure the spectral distribution of optical absorption due to oxyhemoglobin, deoxyhemoglobin, and IRDye800-c(KRGDf). Figure 2(a) shows an *in vivo* pseudocolor functional PAT image of the oxygen saturation of hemoglobin. A focal region pointed by the arrow shows lower oxygen satu-

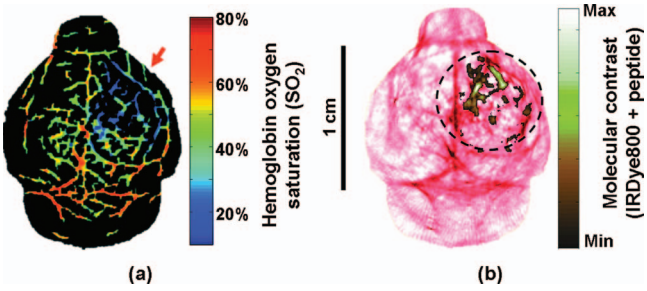


FIG. 2. (a) *In vivo* functional PAT image of hemoglobin in a nude mouse brain with a U87 glioblastoma xenograft. The arrow indicates the hypoxic region. (b) *In vivo* molecular PAT image of tail-vein injected IRDye800-c(KRGDf) in the same nude mouse brain. The circle indicates the region of integrin overexpression. Reproduced with permission (Figs. 2 and 3 of Ref. 31).

ration of hemoglobin than the surrounding area, indicating hypoxia characteristic of tumor due to hypermetabolism. Figure 2(b) shows an *in vivo* pseudocolor molecular PAT image of the molecular imaging probe. Integrin $\alpha_v\beta_3$ is known to overexpress in U87 glioblastoma tumors while IRDye800-c(KRGDf) is known to bind to $\alpha_v\beta_3$ integrin. The circled region indicates the overexpression of integrin in the U87 glioblastoma tumor. The focal regions of both the functional and molecular contrasts were corroborated to be the tumor region through postmortem fluorescence imaging and histological examination.

PAT is competitive in sensitivity compared with other existing molecular imaging technologies. In comparison to the nM–pM sensitivity of positron emission tomography at mm spatial resolution, PAT has poorer sensitivity ($\mu$M–nM) but better spatial resolution. While positron emission tomography uses ionizing radiation, PAT uses nonionizing light and ultrasound. Even at its current level, the sensitivity of PAT is superior to that of magnetic resonance imaging (mM). Furthermore, the sensitivity of PAT can be potentially improved by increasing the local optical fluence, increasing the optical absorption cross section of the contrast agent, increasing the photoacoustic conversion efficiency, increasing signal averaging, and sacrificing the spatial resolution. In comparison to pure ultrasound imaging, which measures mechanical contrast, PAT dominantly measures optical contrast and has many choices of contrast agents. Ultrasound molecular imaging, based on microbubbles, is confined to intravascular space only. It is worth mentioning that x-ray imaging has not yet been demonstrated to provide molecular imaging because of its low sensitivity.

In summary, PAT represents a new paradigm for functional and molecular imaging. Translation to the clinic is expected to follow the availability of molecular contrast agents for human use. By combining functional and molecular imaging in PAT, unprecedentedly high sensitivity and specificity of cancer diagnosis are expected.

### III.E. Photoacoustic tomography of gene expressions

Prediction 5: Deep penetrating high-resolution photoacoustic tomography will become a complementary tool to conventional optical imaging of reporter genes.

Understanding the nature of genes during *in vivo* development and pathogenesis is of significant interest. Such understanding can be enabled by gene expression imaging, a form of molecular imaging based on reporter genes. A reporter gene is a segment of DNA fused to another gene of interest. Unlike the contrast-carrying molecular imaging probe presented in the preceding section, reporter genes must express into protein products to provide contrast. The two fused genes, sharing the same promoter, are transcribed into a single mRNA molecule, which is then translated into fused proteins. The protein encoded by the reporter gene carries contrast either directly or through enzymatic reactions. As a result, a positive contrast in a gene expression image indicates up-regulations of both the reporter gene and the fused gene. Alternatively, a reporter gene can be used without gene fusion in order to assay the activity of a particular promoter in a cell. If the promoter is ubiquitous, a reporter gene can be used to tag cells. The most widely used conventional optical imaging of reporter genes include fluorescence imaging of green fluorescence proteins or their mutants[41] and bioluminescence imaging of luciferases.[42]

Molecular PAT of reporter gene lacZ was demonstrated in living rats.[30] The lacZ gene encodes enzyme $\beta$-galactosidase. The enzyme can cleave an optically transparent substrate 5-bromo-4-chloro-3-indolyl-$\beta$-D-galactoside (x-gal), yielding a stable dark blue product. The blue product increases optical absorption and serves as a contrast agent for PAT. So far, x-gal was injected locally because systemic delivery through the tail vein turned out to be inefficient.

We hope to collaborate with developers of reporter genes to construct optical-absorption-based reporter gene systems that are more suitable for PAT. Because of its high spatial resolution at depths beyond the reach of pure high-resolution optical imaging, PAT is expected to become a complementary tool to conventional optical imaging of reporter genes *in vivo*.

### III.F. Doppler photoacoustic tomography

Prediction 6: Doppler photoacoustic tomography will provide imaging of blood flow *in vivo* with high spatial and velocity resolution.

The photoacoustic Doppler effect was recently discovered experimentally.[43,44] While the optical Doppler effect involves light only, the acoustic Doppler effect involves sound only. By contrast, the photoacoustic Doppler effect involves both light and sound, resulting from the combination of the photoacoustic and Doppler effects. Here, the photoacoustic wave undergoes a Doppler shift when the photoacoustic source—the part of the light absorbing medium generating the photoacoustic wave—has motion relative to the acoustic detector.

An important application is to image blood flow *in vivo* by measuring the photoacoustic Doppler effect due to moving red blood cells. We coined photoacoustic Doppler flowmetry (PADF) for this imaging technology. PADF has potential advantages over conventional Doppler flowmetry. First, PAT can image blood vessels at a depth of a few millimeters with a spatial resolution of tens of micrometers, whereas Doppler optical coherence tomography can penetrate only one optical transport mean free path. Second, PADF tracks light absorbing particles instead of scattering particles. Because red blood cells have much higher optical absorption than the background outside blood vessels, PADF should have low background noise and high sensitivity. By contrast, acoustic flowmetry suffers from background scattering and consequently has difficulty measuring slow flows. Third, the Doppler shift in PADF is nearly independent of the excitation light, enabling accurate measurement of both speed and direction of flow even at large depths inside an optically scattering medium. In comparison, laser Doppler flowmetry suffers from multiple light scattering, limiting the sensing depth and obscuring the information of flow direction. Finally,

PADF is free of speckle artifacts. Therefore, PADF is expected to break fresh ground for *in vivo* flow measurement with high spatial resolution and high velocity sensitivity.

### III.G. Photoacoustic tomography of metabolic rate of oxygen

Prediction 7: Photoacoustic tomography will become the first single modality that can independently image the metabolic rate of oxygen *in vivo* using endogenous contrast.

The metabolic rate of oxygen ($MRO_2$) quantifies metabolism, which can potentially be directly used to measure hypermetabolism, a hallmark of cancer. The $MRO_2$ is defined as the amount of oxygen consumed in a given tissue region per unit time per 100 g of tissue or of the organ of interest. Because in typical physiological conditions, hemoglobin is the dominant carrier of oxygen the key measure of blood oxygenation is oxygen saturation of hemoglobin ($SO_2$).

PAT can simultaneously image cross sections of blood vessels, the concentration and oxygenation of hemoglobin, as well as blood flow *in vivo*. These four parameters suffice to quantify oxygen metabolism in tissues and organs. For a single-vessel system, we have

$$\mathrm{MRO}_2 \propto (\mathrm{SO}_2^{\mathrm{in}} - \mathrm{SO}_2^{\mathrm{out}}) \cdot C_{\mathrm{Hb}} \cdot A_{\mathrm{in}} \cdot \bar{\nu}_{\mathrm{in}}. \quad (1)$$

Here, $A_{\mathrm{in}}$ is the area of the incoming vessel, $\bar{\nu}_{\mathrm{in}}$ is the mean flow velocity of blood in the incoming vessel, $C_{\mathrm{Hb}}$ is the total concentration of hemoglobin, $\mathrm{SO}_2^{\mathrm{in}}$ is the $SO_2$ of the incoming vessel to the region of interest, and $\mathrm{SO}_2^{\mathrm{out}}$ is the $SO_2$ of the outgoing vessel. While $A_{\mathrm{in}}$ is measured by structural PAT, $C_{\mathrm{Hb}}$ and $SO_2$ are measured by multiwavelength functional PAT; further, $\bar{\nu}_{\mathrm{in}}$ is estimated using Doppler photoacoustic flowmetry.

It is extremely fortuitous that all independent parameters in Eq. (1) can be measured by PAT, a single hybrid imaging modality. By contrast, magnetic resonance imaging detects only temporal changes in deoxyhemoglobin concentration instead of absolute values. Equation (1) can be extended to a multivessel system. Although positron emission tomography can image $MRO_2$, exogenous radioactive tracers are required.[45,46] Diffuse optical tomography has also been used to image $MRO_2$ except that a theoretical model or another technique (diffuse correlation imaging) is needed to estimate the blood flow.[47,48] Further, both positron emission tomography and diffuse optical tomography have low spatial resolution. Therefore, PAT will potentially become the first single modality that can independently image the metabolic rate of oxygen *in vivo* at high spatial resolution without the use of exogenous contrast agent. It is expected to play a critical role in metabolism-related biomedical research and clinical diagnosis.

### III.H. Sentinel lymph node mapping using photoacoustic tomography

Prediction 1: Sentinel lymph node mapping will become one of the first niche applications of photoacoustic tomography.

For patients with breast cancer but clinically negative axillae, biopsy of the sentinel lymph node (SLN)—the first draining nodes—for axillary staging has become a standard clinical practice. In this conventional method, both optical dye and radioactive Tc-99 colloids are injected into the breast tumor. Both contrast agents are accumulated by SLNs. Emission from radioactivity is first detected to locate approximately the SLNs. Then, the SLNs are located precisely through an invasive surgical procedure by visually tracing the accumulated optical dye such as methylene blue. The identified SLNs are then resected for pathological examination. Unfortunately, the surgical procedure has associated morbidity. A noninvasive method for accurately locating the SLN *in vivo* is sought-after because noninvasive diagnostic methods such as fine needle biopsy could be subsequently utilized without surgery.

PAT can potentially map the SLN noninvasively with high spatial resolution in real time, avoiding invasive surgery and harmful radioactivity. Preliminary data demonstrated that PAT has both the required penetration depth and spatial resolution for SLN mapping.[49] PAT can identify whether a node is sentinel by detecting the accumulated dye because the dye has high optical absorption contrast. The peak absorption wavelength of methylene blue dye is 690 nm, which lies near the optimal optical penetration window. Since the optical contrast agent has been used in clinical SLN biopsy already, avoiding FDA approval for a new optical contrast agent can significantly accelerate the translation of PAT into the clinic.[50] While PAT has broad potential applications, imaging the SLN is a perfect niche clinical application of PAT with anticipated high impact on breast axillary staging and management.

### III.I. Multiscale photoacoustic imaging *in vivo* with common signal origins

Prediction 9: Multiscale photoacoustic tomography of the same signal origins *in vivo* will enable research in multiscale biology.

Multiscale biology, recognized as the future of biomedical sciences, needs multiscale imaging. To understand the workings of a whole biological system, components spanning multiple spatial scales must be integrated. The components may range from subcellular organelles (sub-$\mu$m scale), through cells ($\mu$m), to organs (cm). To facilitate research in multiscale biology, we must provide multiscale imaging *in vivo* with common signal origins. If the contrast mechanisms were disconnected among the images of various length scales, integrating discoveries across the scales would be challenging.

PAT can provide multiscale imaging *in vivo* with the same contrast origins (Fig. 3). Our original 50-MHz photoacoustic microscope can penetrate 3 mm at tens of $\mu$m resolution. The image resolution and the penetration limit are scalable with the ultrasonic frequency within the reach of photons. On the one hand, the penetration limit can be scaled up to centimeters, i.e., the hard depth limit. In this case, photoacoustic microscopy is scaled to macroscopy. For example,

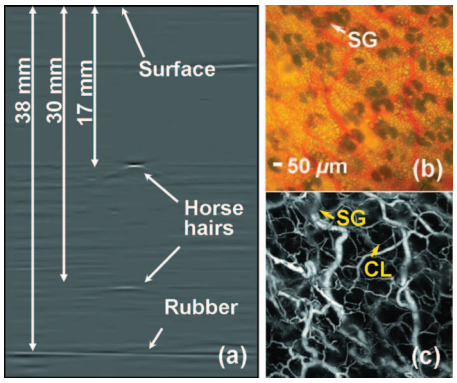


FIG. 3. (a) Image acquired with the 5-MHz photoacoustic imaging system showing the 30 mm penetration limit in chicken breast tissue. Reproduced with permission (Fig. 2) (Ref. 51). (b) Photograph taken with transmission optical microscopy showing the microvasculature in a nude mouse ear. (c) *In vivo* photoacoustic image of the vasculature acquired with optical-resolution photoacoustic microscopy. CL: capillary; SG: sebaceous gland. Reproduced with permission (Fig. 3 of Ref. 52).

employing a 5-MHz ultrasonic transducer and an 804-nm light source scaled the penetration to 3 cm as shown in Fig. 3(a).[51] On the other hand, the spatial resolution can be scaled down to $<10$ $\mu$m. Using a focused light beam resulted in 5 $\mu$m lateral resolution, which is limited by the focal diameter of the excitation light beam. This resolution allows *in vivo* imaging of capillaries—the smallest blood vessels—as shown in Fig. 3(c).[52] Of course, optical focusing is effective only within the soft depth limit. Theoretically, the ultimate spatial resolution is optically diffraction limited, potentially yielding sub-$\mu$m resolution in PAT. Therefore, PAT can potentially image as small as organelles and as large as organs with the same contrast mechanism.

The multiscale or multiresolution capability of PAT is analogous to that of conventional optical microscopy, where a single microscope possesses multiple attached objectives, permitting users to select a magnification factor easily. Such a capability allows one to image a large region of interest at a relatively low resolution. Then, one may zoom into a smaller region of interest with higher resolution to visualize smaller features while the same contrast mechanism is maintained. This scalability is needed because of the tradeoff between the region of interest and the spatial resolution. Of course, such scalability is not limited to a single imaging system. On the contrary, multiple systems can potentially be used to image at various resolution scales.

PAT is uniquely positioned for multiscale imaging *in vivo*. Conventional optical microscopy in various forms is the tool of choice for microscopic imaging of cells and tissues. It is capable of offering a wealth of optical contrasts. PAT extends the depth of conventional optical microscopy beyond the soft depth limit and provides a continuum for multiscale imaging. In comparison, conventional clinical imaging modalities such as x-ray computed tomography, magnetic resonance imaging, positron emission tomography, and single photon emission computed tomography have not been widely used in microscopic form for various reasons. For example, the resolution of positron emission tomography is fundamentally limited by the annihilation range of positrons, on the order of 1 mm. Although ultrasound can achieve microscopic imaging by increasing the frequency from the clinically used MHz range to GHz range, the contrast reflects mechanical rather than biochemical properties. Therefore, PAT is expected to be the first imaging technology, if not the only one on the horizon, that can potentially span a length scale ranging from organelles to organs while providing consistent biochemical contrast.

### III.J. Simultaneous photoacoustic and thermoacoustic tomography of the breast

Prediction 10: Simultaneous photoacoustic and thermoacoustic tomography of the breast will supplement or supplant x-ray mammography.

While breast cancer remains the leading cause of cancer death among women, early diagnosis improves survival. X-ray mammography, the only mass screening tool for detecting nonpalpable breast cancers, has been shown to reduce breast cancer deaths. However, ionizing radiation is required, and detecting dense breasts and early-stage tumors is met with limited sensitivity. In addition, imaging tumors close to the chest wall is difficult. Therefore, alternative nonionizing radiation-based screening technologies are needed. So far, ultrasound imaging has been used as an adjunct to x-ray mammography, especially in differentiating cystic from solid breast masses. Magnetic resonance imaging has high sensitivity but variable specificity. It is further limited by its high cost and use of exogenous contrast agent.

PAT and TAT can be integrated into conventional ultrasound imaging to provide multiple complementary contrasts simultaneously. Three types of images of the breast can be acquired: (1) structural ultrasound pulse-echo images, (2) functional laser-induced PAT images of concentration and oxygen saturation of hemoglobin, and (3) radio frequency-induced TAT images of water and sodium concentrations. Good optical contrast, related to hallmarks of cancer, between tumor and normal breast tissues has been observed.[53] In TAT, up to 5:1 contrast was observed between tumor and normal breast tissues.[29] In comparison, x-ray contrast among soft tissues is typically only a few percent. Again, a single contrast is usually unable to provide accurate diagnosis because of biological variability. However, the combination of multiple complementary measures will likely improve the accuracy.

While compatible with ultrasound imaging, PAT and TAT are also compatible with each other, sharing the same ultrasonic detection system and image reconstruction algorithm. Integrating PAT with TAT adds significant contrast but does not add significant costs. PAT and TAT can potentially be distributed to physicians as an add-on feature to existing clinical ultrasound imaging systems. While PAT and TAT are emerging technologies, ultrasonography is a mature clinical technology. Incorporating PAT and TAT into conventional ultrasonography will facilitate physicians' acceptance of the new technologies.

In summary, PAT and TAT use nonionizing radiation only and can be implemented at relatively low cost. It can potentially provide high-resolution, multicontrast imaging of the breast. Depending on the clinical trial outcome, PAT and TAT could potentially serve as an adjunct or even replace x-ray mammography if its sensitivity and specificity are superior.

### III.K. Photoacoustic and thermoacoustic tomography of the brain

Prediction 11: Photoacoustic and thermoacoustic tomography will provide low-cost, high-resolution, real-time, and even bedside functional imaging of the brain.

Existing high-resolution human brain imaging modalities—including x-ray computed tomography, magnetic resonance imaging, and ultrasonography—have limitations. Both x-ray computed tomography and magnetic resonance imaging are expensive and bulky. Further, x-ray computed tomography uses ionizing radiation, and magnetic resonance imaging requires a strong magnetic field. Therefore, it is advantageous to develop an affordable, nonionizing, high-resolution, and real-time imaging modality that can be used in operating rooms or at the bedside. Such a system can be used to monitor brain functions and conditions such as strokes, head injuries, tumors, and brain infections. In certain cases, ultrasound brain imaging comes close to meeting these objectives. Ultrasonography is an established pediatric brain imaging modality when used before the fontanels are closed. After the closure of the fontanels, the image quality degrades significantly because the skull severely attenuates and distorts ultrasonic waves.

Fortunately, unlike pulse-echo ultrasound imaging, PAT and TAT involve only one-way ultrasound attenuation and distortion due to the skull. As demonstrated previously,[19] ultrasound penetration through small animal skulls is feasible, and the associated distortions are relatively small. The author's group also demonstrated TAT through Rhesus monkey skulls.[54] The extension of PAT and TAT to human brain imaging is an area of research. The primary task is to correct for the phase distortion due to the skull. The skull basically functions as an irregular lens, whose aberration effect can be compensated for if the phase distortion can be quantified. A potential solution is to use geometric measurements of the skull from x-ray computed tomography or magnetic resonance imaging to predict the phase distortion.

PAT and TAT can provide rich contrasts for high-resolution structural and functional imaging. As demonstrated by diffuse optical tomography, near-infrared light can penetrate through the skull to the cortex and has been used for functional brain imaging at low spatial resolution. PAT can potentially provide similar penetration but higher resolution. At an appropriate frequency, radio frequency can penetrate deeper than light. Therefore, TAT can potentially image deeper structures of the brain, while PAT will likely be used to image cortical functions.

PAT and TAT are also relatively low-cost, real-time, and portable. In comparison to x-ray computed tomography and magnetic resonance imaging, ultrasonography is low cost. PAT and TAT essentially involve a laser or radio frequency source in addition to the detection components of an ultrasound imaging system. Therefore, PAT and TAT can be implemented at relatively low cost. When ultrasound arrays are used as in ultrasonography, PAT and TAT can be performed in real time. A standard ultrasound imaging system is portable and can be used at bedside. With the addition of a laser or radio frequency source, the entire imaging system can still be made relatively portable for bedside or operating-room applications. Again, integrating PAT and TAT into existing ultrasound imaging systems can potentially accelerate acceptance of the new technology by physicians.

In summary, the major challenge to PAT and TAT of the human brain is the phase distortion due to the skull. Correcting the distortion is believed to be a tractable problem. Therefore, PAT and TAT are expected to provide low-cost, high-resolution, real-time, and bedside functional imaging of the brain.

### III.L. Low-background thermoacoustic molecular imaging

Prediction 12: Radio frequency-induced thermoacoustic tomography will provide high-resolution, high-sensitivity, and deep-penetrating molecular imaging with the aid of targeted radio frequency contrast agents.

Molecular imaging based on TAT has immense potential. PAT can provide molecular imaging within the hard depth limit for optical imaging. By contrast, radio frequency waves at sufficiently low frequency can penetrate beyond 10 cm as demonstrated in magnetic resonance imaging. Ultrasound at an appropriate frequency can travel a similar depth. Consequently, radio frequency-induced TAT can potentially provide penetration greater than 10 cm. Because low-frequency radiofrequency waves have low absorption, endogenous thermoacoustic signals would be weak, providing a low background. Such a low background enables highly sensitive detection of any other radio frequency absorbers, which can be targeted molecular contrast agents. While PAT boasts a myriad of contrast agents, TAT has none available yet except the recently tested carbon nanotubes.[55] Molecular imaging TAT is somewhat analogous to low-background positron emission tomography except that TAT uses nonionizing radiation and provides high spatial resolution. The author's group is actively seeking collaborations with chemists to identify contrast agents for TAT. Once such contrast agents become available, TAT is expected to avail a new paradigm of high-resolution, low-background, high-sensitivity, and deep-penetrating molecular imaging.

## IV. SUMMARY

The author believes that PAT and TAT will find broad applications in both basic research and clinical care. In general, it can potentially be applied in tumor studies, where angiogenesis and hypermetabolism are highly correlated with cancer aggressiveness; in neuroscience, where oxygen saturation and concentration of hemoglobin are related to neural activities; in radiotherapy and chemotherapy of can-

cer, where hypoxia is responsible for resistance to therapy; and in trauma evaluation, where optical absorption is associated with both hemorrhage and edema.

The aforementioned predictions represent the author's biased opinions of the most promising prospects of PAT and TAT. The topics of the 12 predictions are recapitulated as follows: (1) photoacoustic microscopy of optical absorption emerging as a mainstream technology, (2) melanoma detection using photoacoustic microscopy, (3) photoacoustic endoscopy, (4) simultaneous functional and molecular photoacoustic tomography, (5) photoacoustic tomography of gene expression, (6) Doppler photoacoustic tomography for flow measurement, (7) photoacoustic tomography of metabolic rate of oxygen, (8) photoacoustic mapping of sentinel lymph nodes, (9) multiscale photoacoustic imaging *in vivo* with common signal origins, (10) simultaneous photoacoustic and thermoacoustic tomography of the breast, (11) photoacoustic and thermoacoustic tomography of the brain, and (12) low-background thermoacoustic molecular imaging.

The following specific clinical applications are also worth pursuing: Demarcation of cancer for Mohs surgery, treatment planning, and monitoring for laser therapy of port-wine stains, skin burn imaging to determine the need for skin graft, intraoperative demarcation of brain tumors, and intraoperative imaging of brain functions. Undoubtedly, many more applications will be identified.

While the photoacoustics research community continues to discover new phenomena and invent new technologies, several companies are actively commercializing photoacoustic tomography. We look forward to seeing the impact of PAT and TAT on biomedicine.

## ACKNOWLEDGMENTS

This work is sponsored in part by National Institutes of Health Grant Nos. R01 EB000712 and R01 NS46214 (Bioengineering Research Partnership). L.W. has a financial interest in Endra, Inc., which, however, did not support this work.

[a]Telephone: 314-935-6152; Fax: 314-935-7448. Electronic mail: lhwang@biomed.wustl.edu

[1]M. H. Xu and L. V. Wang, "Photoacoustic imaging in biomedicine," Rev. Sci. Instrum. **77**, 041101 (2006).
[2]L. V. Wang, "Tutorial on photoacoustic microscopy and computed tomography," IEEE J. Sel. Top. Quantum Electron. **14**, 171–179 (2008).
[3]A. A. Oraevsky and L. V. Wang, *Photons Plus Ultrasound: Imaging and Sensing* (SPIE, Bellingham, 2007), Vol. 643.
[4]L. V. Wang and H. Wu, *Biomedical Optics: Principles and Imaging* (Wiley, Hoboken, NJ, 2007).
[5]C. G. A. Hoelen, F. F. M. de Mul, R. Pongers, and A. Dekker, "Three-dimensional photoacoustic imaging of blood vessels in tissue," Opt. Lett. **23**, 648–650 (1998).
[6]L. V. Wang, X. M. Zhao, H. T. Sun, and G. Ku, "Microwave-induced acoustic imaging of biological tissues," Rev. Sci. Instrum. **70**, 3744–3748 (1999).
[7]R. A. Kruger, D. R. Reinecke, and G. A. Kruger, "Thermoacoustic computed tomography—technical considerations," Med. Phys. **26**, 1832–1837 (1999).
[8]A. A. Karabutov, E. V. Savateeva, N. B. Podymova, and A. A. Oraevsky, "Backward mode detection of laser-induced wide-band ultrasonic transients with optoacoustic transducer," J. Appl. Phys. **87**, 2003–2014 (2000).
[9]G. Ku and L. V. Wang, "Scanning electromagnetic-induced thermoacoustic tomography: Signal, resolution, and contrast," Med. Phys. **28**, 4–10 (2001).
[10]K. P. Kostli, D. Frauchiger, J. J. Niederhauser, G. Paltauf, H. P. Weber, and M. Frenz, "Optoacoustic imaging using a three-dimensional reconstruction algorithm," IEEE J. Sel. Top. Quantum Electron. **7**, 918–923 (2001).
[11]M. H. Xu, G. Ku, and L. V. Wang, "Microwave-induced thermoacoustic tomography using multi-sector scanning," Med. Phys. **28**, 1958–1963 (2001).
[12]G. Paltauf, J. A. Viator, S. A. Prahl, and S. L. Jacques, "Iterative reconstruction algorithm for optoacoustic imaging," J. Acoust. Soc. Am. **112**, 1536–1544 (2002).
[13]M. H. Xu and L. V. Wang, "Time-domain reconstruction for thermoacoustic tomography in a spherical geometry," IEEE Trans. Med. Imaging **21**, 814–822 (2002).
[14]Y. Xu, D. Z. Feng, and L. V. Wang, "Exact frequency-domain reconstruction for thermoacoustic tomography-I: Planar geometry," IEEE Trans. Med. Imaging **21**, 823–828 (2002).
[15]Y. Xu, M. H. Xu, and L. V. Wang, "Exact frequency-domain reconstruction for thermoacoustic tomography-II: Cylindrical geometry," IEEE Trans. Med. Imaging **21**, 829–833 (2002).
[16]V. G. Andreev, A. A. Karabutov, and A. A. Oraevsky, "Detection of ultrawide-band ultrasound pulses in optoacoustic tomography," IEEE Trans. Ultrason. Ferroelectr. Freq. Control **50**, 1383–1390 (2003).
[17]D. Finch, S. K. Patch, and Rakesh, "Determining a function from its mean values over a family of spheres," SIAM J. Math. Anal. **35**, 1213–1240 (2003).
[18]K. P. Kostli and P. C. Beard, "Two-dimensional photoacoustic imaging by use of Fourier-transform image reconstruction and a detector with an anisotropic response," Appl. Opt. **42**, 1899–1908 (2003).
[19]X. D. Wang, Y. J. Pang, G. Ku, X. Y. Xie, G. Stoica, and L. V. Wang, "Noninvasive laser-induced photoacoustic tomography for structural and functional *in vivo* imaging of the brain," Nat. Biotechnol. **21**, 803–806 (2003).
[20]X. D. Wang, Y. J. Pang, G. Ku, G. Stoica, and L. V. Wang, "Three-dimensional laser-induced photoacoustic tomography of mouse brain with the skin and skull intact," Opt. Lett. **28**, 1739–1741 (2003).
[21]M. H. Xu and L. V. Wang, "Analytic explanation of spatial resolution related to bandwidth and detector aperture size in thermoacoustic or photoacoustic reconstruction," Phys. Rev. E **67**, 056605 (2003).
[22]M. Haltmeier, O. Scherzer, P. Burgholzer, and G. Paltauf, "Thermoacoustic computed tomography with large planar receivers," Inverse Probl. **20**, 1663–1673 (2004).
[23]G. Ku, X. D. Wang, G. Stoica, and L. V. Wang, "Multiple-bandwidth photoacoustic tomography," Phys. Med. Biol. **49**, 1329–1338 (2004).
[24]Y. Xu and L. V. Wang, "Time reversal and its application to tomography with diffracting sources," Phys. Rev. Lett. **92**, 033902 (2004).
[25]B. T. Cox and P. C. Beard, "Fast calculation of pulsed photoacoustic fields in fluids using k-space methods," J. Acoust. Soc. Am. **117**, 3616–3627 (2005).
[26]G. Ku and L. V. Wang, "Deeply penetrating photoacoustic tomography in biological tissues enhanced with an optical contrast agent," Opt. Lett. **30**, 507–509 (2005).
[27]G. Ku, X. D. Wang, X. Y. Xie, G. Stoica, and L. V. Wang, "Imaging of tumor angiogenesis in rat brains *in vivo* by photoacoustic tomography," Appl. Opt. **44**, 770–775 (2005).
[28]J. Zhang, M. A. Anastasio, X. C. Pan, and L. V. Wang, "Weighted expectation maximization reconstruction algorithms for thermoacoustic tomography," IEEE Trans. Med. Imaging **24**, 817–820 (2005).
[29]G. Ku, B. D. Fornage, X. Jin, M. H. Xu, K. K. Hunt, and L. V. Wang, "Thermoacoustic and photoacoustic tomography of thick biological tissues toward breast imaging," Technol. Cancer Res. Treat. **4**, 559–565 (2005).
[30]L. Li, R. J. Zemp, G. Lungu, G. Stoica, and L. V. Wang, "Photoacoustic imaging of lacZ gene expression *in vivo*," J. Biomed. Opt. **12**, 020504-(1–3) (2007).
[31]M. Li, J. Oh, X. Xie, G. Ku, W. Wang, C. Li, G. Lungu, G. Stoica, and L. V. Wang, "Simultaneous molecular and hypoxia imaging of brain tumors *in vivo* using spectroscopic photoacoustic tomography," Proc. IEEE **96**, 481–489 (2008).
[32]L. V. Wang and G. Liang, "Absorption distribution of an optical beam focused into a turbid medium," Appl. Opt. **38**, 4951–4958 (1999).

[33]K. Maslov, G. Stoica, and L. V. Wang, "*In vivo* dark-field reflection-mode photoacoustic microscopy," Opt. Lett. **30**, 625–627 (2005).
[34]H. F. Zhang, K. Maslov, G. Stoica, and L. V. Wang, "Functional photoacoustic microscopy for high-resolution and noninvasive *in vivo* imaging," Nat. Biotechnol. **24**, 848–851 (2006).
[35]H. F. Zhang, K. Maslov, and L. V. Wang, "*In vivo* imaging of subcutaneous structures using functional photoacoustic microscopy," Nature Protocols **2**, 797–804 (2007).
[36]M. H. Xu and L. V. Wang, "Universal back-projection algorithm for photoacoustic computed tomography," Phys. Rev. E **71**, 016706 (2005).
[37]B. T. Cox, S. R. Arridge, K. P. Kostli, and P. C. Beard, "Two-dimensional quantitative photoacoustic image reconstruction of absorption distributions in scattering media by use of a simple iterative method," Appl. Opt. **45**, 1866–1875 (2006).
[38]R. J. Zemp, R. Bitton, M. L. Li, K. K. Shung, G. Stoica, and L. V. Wang, "Photoacoustic imaging of the microvasculature with a high-frequency ultrasound array transducer," J. Biomed. Opt. **12**, 010501-(1–3) (2007).
[39]R. J. Zemp, L. Song, R. Bitton, K. K. Shung, and L. V. Wang, "Realtime photoacoustic microscopy *in vivo* with a 30-MHz ultrasound array transducer," Opt. Express **16**, 7915–7928 (2008).
[40]S. Sethuraman, J. H. Amirian, S. H. Litovsky, R. W. Smalling, and S. Y. Emelianov, "*Ex vivo* characterization of atherosclerosis using intravascular photoacoustic imaging," Opt. Express **15**, 16657–16666 (2007).
[41]R. Y. Tsien, "The green fluorescent protein," Annu. Rev. Biochem. **67**, 509–544 (1998).
[42]C. H. Contag and M. H. Bachmann, "Advances *in vivo* bioluminescence imaging of gene expression," Annu. Rev. Biomed. Eng. **4**, 235–260 (2002).
[43]H. Fang, K. Maslov, and L. V. Wang, "Photoacoustic Doppler effect from flowing small light-absorbing particles," Phys. Rev. Lett. 99, 184501-(1–4) (2007).
[44]H. Fang, K. Maslov, and L. V. Wang, "Photoacoustic Doppler flow measurement in optically scattering media," Appl. Phys. Lett. **91**, 264103–264101 (2007).
[45]N. Kudomi, H. Watabe, T. Hayashi, and H. Iida, "Separation of input function for rapid measurement of quantitative CMRO2 and CBF in a single PET scan with a dual tracer administration method," Phys. Med. Biol. **52**, 1893–1908 (2007).
[46]S. H. Yee, K. Lee, P. A. Jerabek, and P. T. Fox, "Quantitative measurement of oxygen metabolic rate in the rat brain using microPET imaging of briefly inhaled O-15-labelled oxygen gas," Nucl. Med. Commun. **27**, 573–581 (2006).
[47]D. A. Boas, G. Strangman, J. P. Culver, R. D. Hoge, G. Jasdzewski, R. A. Poldrack, B. R. Rosen, and J. B. Mandeville, "Can the cerebral metabolic rate of oxygen be estimated with near-infrared spectroscopy?," Phys. Med. Biol. **48**, 2405–2418 (2003).
[48]J. P. Culver, T. Durduran, T. Furuya, C. Cheung, J. H. Greenberg, and A. G. Yodh, "Diffuse optical tomography of cerebral blood flow, oxygenation, and metabolism in rat during focal ischemia," Biopolymers **23**, 911–924 (2003).
[49]K. H. Song, E. W. Stein, J. A. Margenthaler, and L. V. Wang, "Noninvasive photoacoustic identification of sentinel lymph nodes containing methylene blue *in vivo* in a rat model," J. Biomed. Opt. **13**, 054033-(1–6) (2008).
[50]E. M. Sevick-Muraca, R. Sharma, J. C. Rasmussen, M. V. Marshall, J. A. Wendt, H. Q. Pham, E. Bonefas, J. P. Houston, L. Sampath, K. E. Adams, D. K. Blanchard, R. E. Fisher, S. B. Chiang, R. Elledge, and M. E. Mawad, "Imaging of lymph flow in breast cancer patients after microdose administration of a near-infrared flurophore: Feasibility study," Radiology **246**, 734–741 (2008).
[51]K. Song and L. V. Wang, "Deep reflection-mode photoacoustic imaging of biological tissue," J. Biomed. Opt. **12**, 060503 (2007).
[52]K. Maslov, H. F. Zhang, S. Hu, and L. V. Wang, "Optical-resolution photoacoustic microscopy for *in vivo* imaging of single capillaries," Opt. Lett. **33**, 929–931 (2008).
[53]Q. Zhu, C. Xu, P. Y. Guo, A. Aquirre, B. H. Yuan, F. Huang, D. Castilo, J. Gamelin, S. Tannenbaum, M. Kane, P. Hedge, and S. Kurtzman, "Optimal probing of optical contrast of breast lesions of different size located at different depths by US localization," Technol. Cancer Res. Treat. **5**, 365–380 (2006).
[54]Y. Xu and L. V. Wang, "Rhesus monkey brain imaging through intact skull with thermoacoustic tomography," IEEE Trans. Ultrason. Ferroelectr. Freq. Control **53**, 542–548 (2006).
[55]M. Pramanik, M. Swierczewska, D. Green, B. Sitharaman, and L. V. Wang, "Carbon nanotubes as a multimodal—thermoacoustic and photoacoustic—contrast agent" (unpublished).